Saturn’s rings spectrophotometric modeling by CASSINI-VIMS data

M.Ciarniello[1], F. Capaccioni[1], G. Filacchione[1], P.D. Nicholson[2], R. N. Clark[3], P. Cerroni[1], A. Coradini[4], R. H. Brown[5], B. J. Buratti[6], M. M. Hedman[2]

[1]INAF-IASF, via del Fosso del Cavaliere, 100, Rome, Italy (mauro.ciarniello@iasf-roma.inaf.it); [2]Department of Astronomy, Cornell University, Ithaca, NY 14853, USA; [3]U.S. Geological Survey, Denver, CO, USA; [4]INAF-IFSI, via del Fosso del Cavaliere, 100, Rome, Italy; [5]Lunar and Planetary Lab and Steward Observatory, University of Arizona, Tucson, AZ, USA; [6]Jet Propulsion Laboratory, California Institute of Technology, Pasadena, CA, USA.

Introduction

VIMS (Visual Infrared Mapping Spectrometer) is an imaging spectrometer onboard the Cassini spacecraft. It produces monochromatic images of the target in 352 bands covering the 0.35 - 5.12 μm range using two channels: VIS and IR (fig. 1) [1]. During seven years spent orbiting in the Saturn system more than 54000 hyperspectral cubes of the rings have been produced. This huge amount of data allows to study their spectral properties. Spectra and phase curve can be interpreted through radiative transfer models, which allow to infer surface properties of the target, such as particles grain size, amount of contaminants and particles photometric characteristics.

Following the approach applied in [2] on Rhea, in this paper we investigate the main rings of Saturn, applying the Hapke model for a semi-infinite medium [3] adapted to a finite optical depth layer of particles.

The Saturn rings system is the most extensive in the Solar System. It extends from 66900 to 480000 km from Saturn center and the main rings are (in order of distance from the planet) D,C,B,A,F,G and E. The two densest regions are the B and A rings, which are divided by an underdense region named Cassini Division (CD). The vertical extent of the rings is of the order of tenth’s of meters with particle sizes ranging from few centimeters to 10 meters.

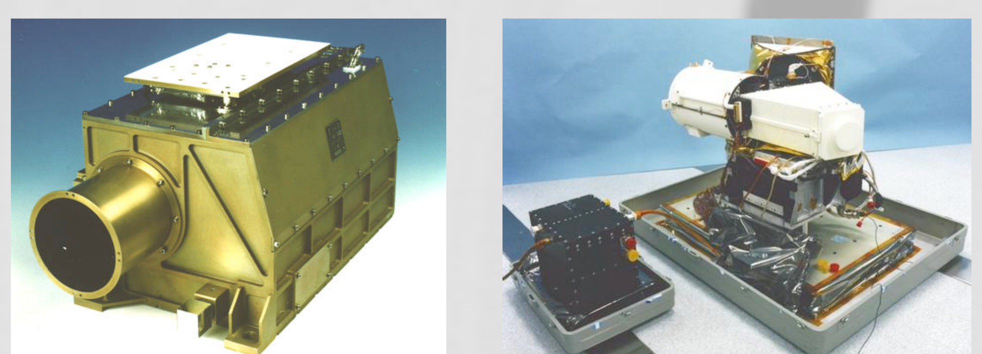

Fig.1 VIMS imaging spectrometer: VIS channel (left), IR channel (right)

Dataset

The analyzed dataset is composed of 312 hyperspectral cubes covering the ring plane up to the F ring. Illumination conditions (incidence angle, emission angle and phase angle) change over the entire dataset, and the target-spacecraft distance as well. Moreover cubes acquired in both “NORMAL” and “HIGH RESOLUTION” modes have been considered. In order to localize each observation on the rings plane a geometric reprojection of the whole dataset has been performed. Each pixel has been labeled with 6 parameters: radial distance on the ring plane, azimuth angle on the ring plane, Cassini-target distance, incidence angle,emission angle and phase angle. In fig. 2 the entire dataset reprojected on the rings is plotted, both for VIS and IR channels.

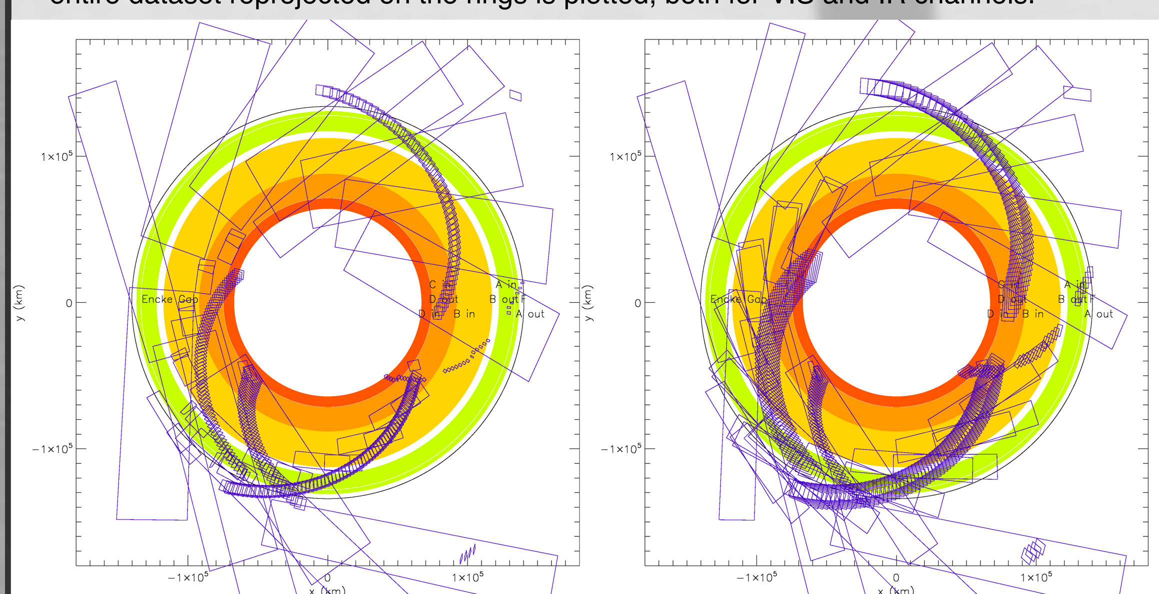

Fig.2 Geometric reprojection of the dataset on the rings plane: VIS (left) and IR (right)

VIS and IR can show some differences due to the different instant field of view (IFOV) of the two channels in HIGH-RESOLUTION mode (VIS IFOV=167μrad X 167μrad, IR IFOV=250μrad X 500μrad). In fig. 3 the radial distance against phase angle is plotted for pixel of the VIS channel whose maximum linear size on the ring plane is <3000 km (For the IR channel the spatial resolution can be three times worse). For spectral analysis only pixels with VIS resolution comprised in the 500-1000 km range have been considered.

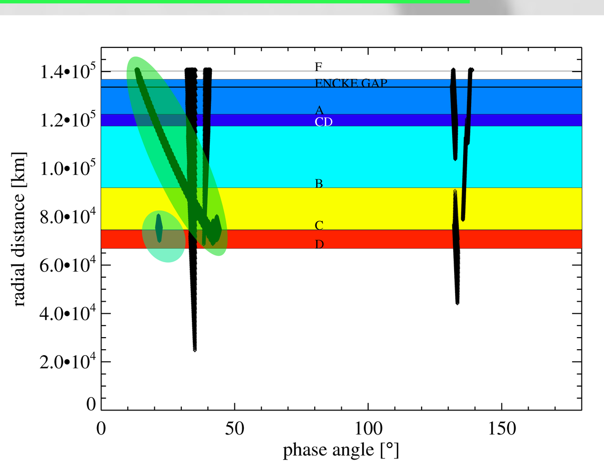

Fig.3 Radial distance vs. phase angles for pixel with linear size on the ring <3000 km (VIS channel). Pixels with linear size in the 500-1000 km range are rimmed.

Model

Spectral analysis of Saturn rings in VIS-IR show that spectral signatures (e.g. water ice bad depths) are due to particles whose size is in 10 μm-1000 μm [4]. These sizes are smaller than the typical size of the icy chunks composing the rings (10 cm - 10 m). This means that the signal we are receiving is mostly due to regolith covering the blocks. We approximate the behavior of the these icy chunks to a semi-infinite medium applying the equation of bidirectional reflectance from Hapke (1993):

$$r(\mu_0,\mu,g)=\frac{w}{4\pi}\frac{\mu_0}{\mu+\mu_0}\left\{p(g)\left[1+B(g)\right]+H(\mu_0)H(\mu)\right\}S\left(i,e,g\right)$$

$$\mu=\cos e$$

$$\mu_0=\cos i$$

In the above equation *i,e* and *g* are respectively the incidence, emission and phase angle, *w* the single scattering albedo, *p(g)* the single particle phase function and *H(x)* the Chandrasekhar function. *B(g)* describes the opposition effect and *S(i,e,g)* takes into account for large scale surface roughness.

In order to consider the different densities of the various regions of the rings we need to multiply this equation for:

$$(1-e^{-(1/\mu_0+1/\mu)\tau})$$

where τ is the optical depth. This term represents the probability for a light ray to interact with the rings at optical depth τ and to escape toward the observer.

For the rings case we can neglect surface roughness and if we observe at g >15-20° (far from opposition surge) the final equation which describes the rings I/F is:

$$\frac{I}{F}=\frac{w}{4}\frac{1}{\mu_0+\mu}\left[p(g)+H(\mu_0)H(\mu)\right]\left(1-e^{-(1/\mu_0+1/\mu)\tau}\right)$$

In this framework multiple scattering between icy chunks is neglected, while we take into account for multiple scattering of regolith on the surface of the blocks. This approach has two major limits: it doesn’t take into account for small isolated particles and considers the scattering surface of the icy chunks parallel to the ring plane. The last assumption allows to use ring incidence and emission angles (fig. 4).

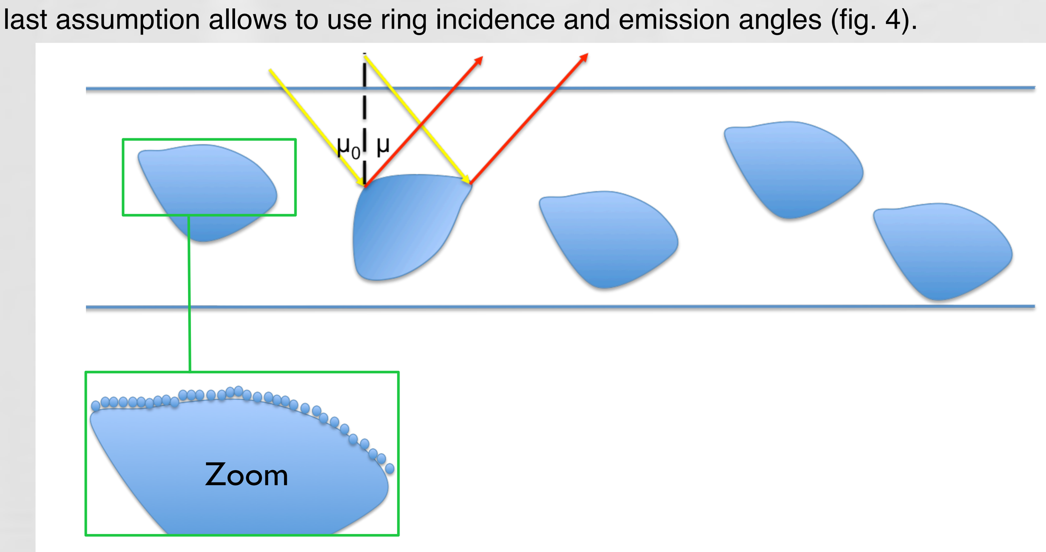

Fig.4 Schematic representation of the rings. Incident and emitted rays are plotted

Spectral fit

Single scattering albedo

Single scattering albedo is computed at each wavelength following the Hapke model. It depends on the grain size distribution of icy particles and on the abundance, type and mixing of contaminants. We investigated four reddish organic compounds as contaminant, in order to produce the UV downturn in rings spectra:

- Amorphous carbon [5]
- Triton tholin [6]
- Titan tholin [6]
- Tholin from Khare et al. 1993 [7]

Areal, intimate and intraparticle [8] ice-contaminant mixtures have been examined with various grain size distributions: monodisperse,uniform, power law and lognormal.

Single particle phase function

The single particle phase function *p(g)* is an important quantity to establish the absolute albedo level of the spectrum. Moreover it depends on wavelength. Its value can be computed through Mie theory for a spherical isolated particle. In close-packed media Mie results cannot be applied unless the forward scattering lobe due to diffraction is removed and the phase function is renormalized.This procedure is quite long and suffers the assumption of a perfect spherical shape of the grain which is not the case of a real icy particle. However in Mie calculations a correlation between single particle phase function at given phase angle and single scattering albedo is shown. This correlation is positive in the range we are studying (20°-40°) (fig. 5). For this reason we found an empirical expression for the single particle phase function, where a spectral dependence with single scattering albedo is introduced:

$$p(g)=1.5\sqrt{w}$$

The dependence on the root of *w* comes out from the spectral fit attempts.

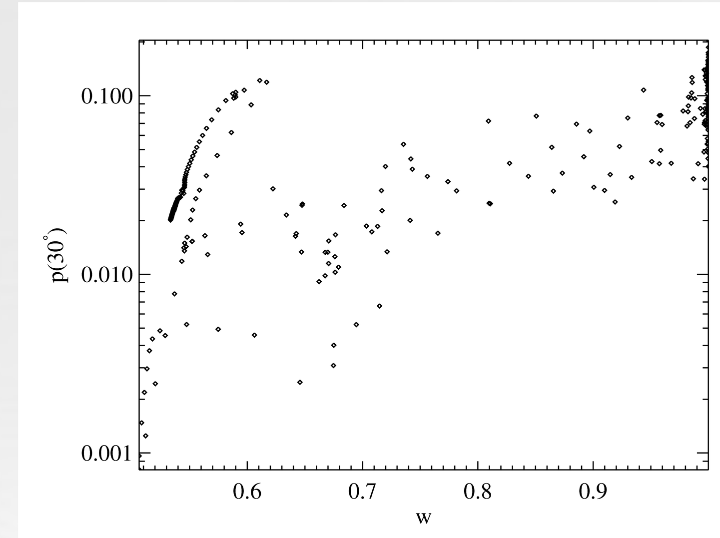

Fig.5 Mie calculation of single particle phase function at g=30° vs. single scattering albedo for a 200μm size particle with inclusion of Triton tholin (0.4%). The calculation is performed at VIMS wavelengths.

Optical depth

Optical depth for the investigated region of the rings has been averaged from Voyager PPS and UVS data on the Planetary Rings Node (http://pds-rings.seti.org). VIMS wavelengths are smaller than the tipical size of icy chunks on the rings so optical depth values don’t depend on wavelength.

Results

C ring (fig. 5)

The final spectrum is an average of 248 spectra for the VIS channel and 305 for the IR with the following properties:

- radial distance from Saturn center: 80000-81000 km
- average incidence: 111°.6; average emission angle: 99°.9
- average phase angle: 37°.5
- optical depth: 0.0092

The best fit is given by an intimate mixture of two species of particles: *A* (35%) and *B* (65%). *A* particles are an intraparticle mixture of water ice (99.8%) and Triton tholin (0.2%). *B* particles are an intraparticle mixture of water ice (98.7%) and amorphous carbon (1.3%). The grain size (*a*) distribution is a power law ($\propto a^{-q}$) with *q=3*, minimum size a_m = 20 μm and maximum size a_M = 600 μm.

B ring (fig. 6)

The final spectrum is an average of 285 spectra for the VIS channel and 417 of the IR with the following properties:

- radial distance from Saturn center: 102000-103000 km
- average incidence: 111°.6; average emission angle: 102°.7
- average phase angle: 27°.0
- optical depth: 1.65

The best fit is given by an intimate mixture of two species of particles: *A* (96.5%) and *B* (3.5%). *A* particles are an intraparticle mixture of water ice (99.5%) and Triton tholin (0.5%). *B* particles are made of amorphous carbon. The grain size (*a*) distribution is a power law ($\propto a^{-q}$) with *q=3*, minimum size a_m = 20 μm and maximum size a_M = 700 μm.

Cassini Division (fig. 7)

The final spectrum is an average of 474 spectra for the VIS channel and 436 of the IR with the following properties:

- radial distance from Saturn center: 118000-119000 km
- average incidence: 111°.6; average emission angle: 104°.2
- average phase angle: 20°.7
- optical depth: 0.133

The best fit is given by an intimate mixture of two species of particles: *A* (75%) and *B* (25%). *A* particles are an intraparticle mixture of water ice (99.6%) and Triton tholin (0.4%). *B* particles are an intraparticle mixture of water ice (98.4%) and amorphous carbon (1.6%). The grain size (*a*) distribution is a power law ($\propto a^{-q}$) with *q=3*, minimum size a_m = 14 μm and maximum size a_M = 400 μm.

A ring (fig. 8)

The final spectrum is an average of 310 spectra for the VIS channel and 381 of the IR with the following properties:

- radial distance from Saturn center: 128000-129000 km
- average incidence: 111°.6; average emission angle: 105°.0
- average phase angle: 17°.2
- optical depth: 0.4185

The best fit is given by an intimate mixture of two species of particles: *A* (88%) and *B* (12%). *A* particles are an intraparticle mixture of water ice (99.6%) and Triton tholin (0.4%). *B* particles are made of amorphous carbon. The grain size (*a*) distribution is a power law ($\propto a^{-q}$) with *q=3* and minimum size a_m = 20 μm and maximum size a_M = 700 μm.

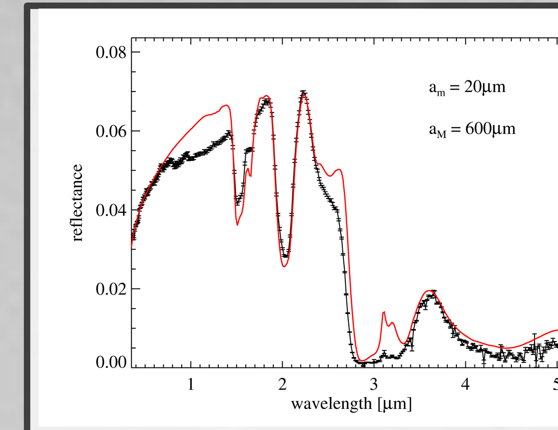

Fig.5 C ring spectrum (black) and best fit (red).

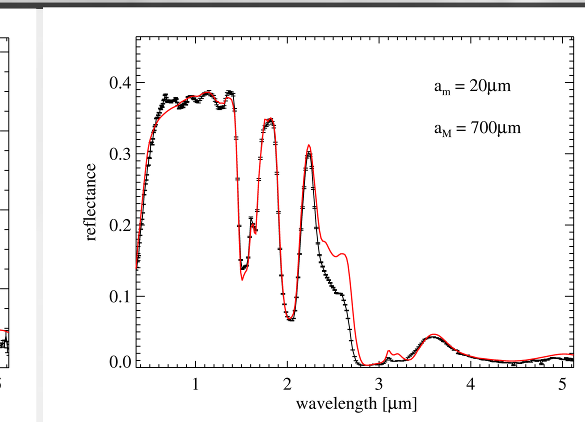

Fig.6 B ring spectrum (black) and best fit (red).

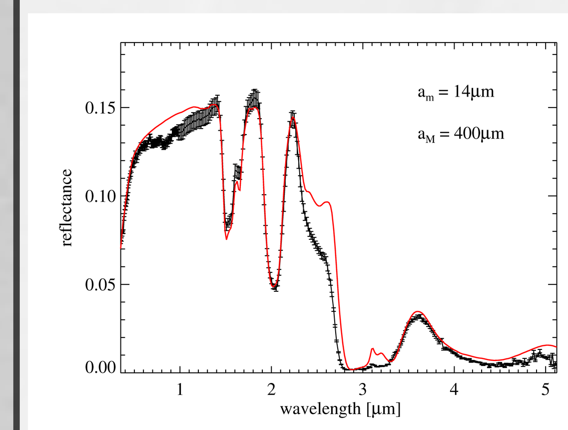

Fig.7 Cassini Division spectrum (black) and best fit (red).

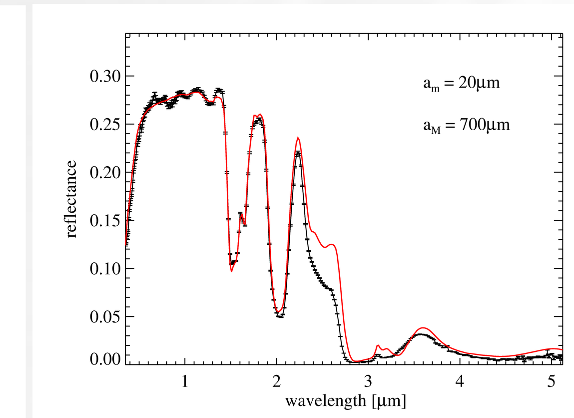

Fig.8 A ring spectrum (black) and best fit (red).

Comparison with Rhea

The results obtained for the rings can be compared with the ones obtained on Rhea (fig. 9) in [2]. The UV downturn is a common propriety of rings and icy satellites, and can explained with an intraparticle mixture of water ice and Trithon (less than 1 %). The brighter rings show a similar behavior to Rhea in the region around 1μm, while the darker rings exhibit a strong reddening. Grain size of Rhea particles constrained by the spectral fit is smaller than the one of the rings (moreover requires a monodisperse distribution instead of a power law). This difference in the grain size distributon is confirmed by the absence of Frenel peak in Rhea spectrum.

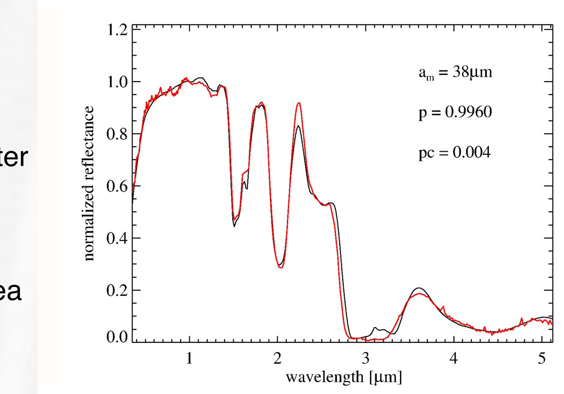

Fig.9 Rhea spectral fit. The model is an intraparticle mixture of water ice (99.6%) and Triton tholin (0.4%) and particle grain size a_m = 38 μm.

Conclusions

- Our best models of the rings are represented by intraparticle mixtures of water ice and organic contaminants with a power-law grain size distribution (fig. 5-6-7-8).

- The UV downturn common to all the rings is well explained by inclusions of Triton tholin in ice particles with tiny amounts (≤ 5%). The model works better for the densest regions (A and B rings), while fails to reproduce the strong reddening around 1 μm of the C ring and Cassini division, that seem to be more contaminated.

- We are not able to reproduce the reflectance at 2.5 μm. This issue can be addressed to the grain size distribution but an important effect is given by the single particle phase function, whose value strongly affects the albedo level and changes with wavelength. The major effects of single-particle phase function can be seen in the Fresnel peak region, where single scattering dominates and the overestimation of *p(g)* leads to a worse fit, particularly for the C ring and Cassini division.

- The comparison with Rhea results shows that the same contaminant with similar abundance produces the reddening at short wavelengths but, there are differences in grain size distributions (fig. 9).

Acknowledgements

This work is supported by an Italian Space Agency (ASI) grant.

References

[1] Brown, R.H., Baines, K.H., Bellucci, G., Bibring, J.-P., Buratti, B.J., Capaccioni, F., Cerroni, P., Clark, R.N., Coradini, A., Cruikshank, D.P., Drossart, P., Formisano, V., Jaumann, R., Langevin, Y., Matson, D.L., McCord, T.B., Mennella, V., Miller, E., Nelson, R.M., Nicholson, P.D., Sicardy, B., Sotin, C., 2004. The Cassini Visual and Infrared Mapping Spectrometer (VIMS) investigation. Space Sci. Rev. 115 (1-4), 111-168.

[2] Ciarniello, M., Capaccioni, F., Filacchione, G., Clark, R. N., Cruikshank, D. P. , Cerroni, P., Coradini, A., Brown, R. H., Buratti, B. J., Tosi, F., Stephan, K., 2011. In preparation.

[3] Hapke, B., 1993. Theory of Reflectance and Emittance Spectroscopy, Topics in remote sensing: 3, Cambridge University Press, Cambridge, UK.

[4]Poulet, F. and Cuzzi, J. N., 2002. The Composition of Saturn’s Rings. Icarus, 160, 350-358.

Clark, R. N., D. P. Cruikshank, R. Jaumann, R. H. Brown, J. M. Curchin, T. M. Hoefen, K. Stephan, C. M. Dalle Ore, B. J. Buratti, G. Filacchione, K. H. Baines, P. D. Nicholson, 2011b, The Composition of Iapetus: Mapping Results from Cassini VIMS, *Icarus*, in review.

[5] Zubko, V.G., Mennella, V., Colangeli, L., Bussoletti, E., 1996. Optical constants of cosmic carbon analogue grains _ I. Simulation of clustering by a modified continuous distribution of ellipsoids. Mon. Not. R. Astron. Soc. 282, 1321-1329.

[6] McDonald, G.D., Thompson, W.R., Heinrich, M., Khare, B.N., Sagan, C., 1994. Chemical investigation of Titan and Triton tholins. Icarus 108, 137-145.

Khare, B.N., Sagan, C., Arakawa, E.T., Suits, R., Callcot, T.A., Williams, M.W., 1984. Optical constants of organic tholins produced in a simulated titanian atmosphere: from soft X-ray to microwave frequencies. Icarus 60, 127-137.

[7] Khare, B.N., Thompson, W.R., Cheng, L., Chyba, C., Sagan, C., Arakawa, E.T., Meisse, C., Tuminello, P.S., 1993. Production and optical constraints of ice tholin from charged particle irradiation of (1:6) C2H6/H2O at 77 K. Icarus 103, 290-300.

[8] Grundy, W.M., 2009. Is the missing utra-red material colorless ice? Icarus 199, 560-563.

venerdì 29 aprile 2011